Synthesis and plasmonic properties of silver and gold nanoshells on polystyrene cores of different size and of gold–silver core–shell nanostructures

Ken-Tye Yong [a,c], Yudhisthira Sahoo [a,b], Mark T. Swihart [a,c,*], Paras N. Prasad [a,b]

[a] *Institute for Lasers, Photonics and Biophotonics, University at Buffalo, The State University of New York, Buffalo, NY 14260-4200, USA*
[b] *Department of Chemistry, University at Buffalo, The State University of New York, Buffalo, NY 14260-4200, USA*
[c] *Department of Chemical and Biological Engineering, University at Buffalo, The State University of New York, Buffalo, NY 14260-4200, USA*

Abstract

Simple methods of preparing silver and gold nanoshells on the surfaces of monodispersed polystyrene microspheres of different sizes as well as of silver nanoshells on free-standing gold nanoparticles are presented. The plasmon resonance absorption spectra of these materials are presented and compared to predictions of extended Mie scattering theory. Both silver and gold nanoshells were grown on polystyrene microspheres with diameters ranging from 188 to 543 nm. The commercially available, initially carboxylate-terminated polystyrene spheres were reacted with 2-aminoethanethiol hydrochloride (AET) to yield thiol-terminated microspheres to which gold nanoparticles were then attached. Reduction of silver nitrate or gold hydroxide onto these gold-decorated microspheres resulted in increasing coverage of silver or gold on the polystyrene core. The nanoshells were characterized using transmission electron microscopy (TEM), scanning electron microscopy (SEM) and UV–vis spectroscopy. By varying the core size of the polystyrene particles and the amount of metal (silver or gold) reduced onto them, the surface plasmon resonance of the nanoshell could be tuned across the visible and the near-infrared regions of the electromagnetic spectrum. Necklace-like chain aggregate structures of gold core–silver shell nanoparticles were formed by reducing silver nitrate onto free citrate-gold nanoparticles. The plasmon resonance absorption of these nanoparticles could also be systematically tuned across the visible spectrum.
© 2006 Elsevier B.V. All rights reserved.

Keywords: Nanoshell; Plasmon resonance; Silver; Gold

1. Introduction

Metal colloids are well-known for their surface plasmon resonance (SPR) properties, which originate from collective oscillation of their conduction electrons in response to optical excitation [1–4]. The SPR frequency of a particular metal colloid sample is different from that of the corresponding metal film and has been shown to depend on particle size [5–7], shape [8,9], and dielectric properties [10], aggregate morphology [11], surface modification [12], and refractive index of the surrounding medium [13]. For example, the SPR peak of 13 nm spherical gold colloids is around 520 nm and that of 5–6 nm silver nanoparticles around 400 nm [14]. The SPR peaks shift to the red depending on the particle shape, state of aggregation, and the surrounding dielectric medium [15]. SPR has been explored for use in fabricating optical filters [16], photon energy transport devices [17], probes for scanning near-field optical microscopy [18], active surfaces for surface-enhanced Raman spectroscopy [19] and fluorescence scattering [20], and chemical or biological sensors [21].

Metal nanoshells have shown tremendous promise for systematic engineering of SPR. These are composite nanoparticles that consist of a dielectric core coated with a few nanometers to a few tens of nanometers of a metal, usually gold or silver [22]. The SPR of these nanoparticles can be varied over hundreds of nanometers in wavelength, across the visible and into the infrared region of the spectrum, by varying the relative dimensions of the core and the shell. Using the Mie scattering theory and controllable colloidal growth chemistry, the optical resonance of a core–shell composite nanoparticle can be "designed"

* Corresponding author. Tel.: +1 716 645 2911x2205; fax: +1 716 645 3822.
E-mail address: swihart@eng.buffalo.edu (M.T. Swihart).

in a predictable manner. Because its surface plasmon resonance occurs at energies distinct from any bulk interband transitions, a silver colloid produces a stronger and sharper plasmon resonance than gold [23]. Also, the plasmon resonance of a solid silver nanoparticle appears at a shorter wavelength than that of gold. This feature can potentially provide a broader range of tunability of the plasmon resonance frequency for silver than for gold. Halas and coworkers have been pioneers in developing metal nanoshells on dielectric microspheres [10]. This wide tunability of optical response has already found applications, in areas from photonics and electronics to biology and medicine.

The preparation of gold nanoshells on both silica and polystyrene cores has been reported. One of the most successful approaches has been the 'seed and grow' method that is further developed in this manuscript. In this approach, the surface of the dielectric core particle is modified so that small gold nanoparticles can be attached to it, and then additional gold is reduced onto these 'seed' particles to produce a complete shell. The best-developed combination is gold nanoshells on silica cores [10,24–26] for which Halas and co-workers [10,27] have developed a procedure to make gold nanoshells on silica treated with (aminopropyl)triethoxysilane. There have been fewer reports of gold shells formed on polystyrene spheres [28], even though polystyrene has some importang potential advantages as the core material. Polystyrene spheres have been particularly useful for the formation of photonic crystals [29]. Their high degree of uniformity makes them relatively easy to self-assemble into a uniform colloidal crystal, and the relatively high refractive index contrast between the spheres and air-filled voids within them allows for enhanced confinement of light [29,30]. The higher refractive index of polystyrene, compared to silica, also can result in a narrower plasmon resonance absorption peak for gold nanoshells on polystyrene, compared to gold nanoshells on silica [31]. Recently, we have synthesized gold nanoshells on polystyrene spheres and demonstrated tuning of the SPR absorption of these shells by varying the amount of gold deposited [31]. In that case, the shell thickness and roughness could be systematically controlled by the size of the gold nanoparticle seeds as well as by the process of their growth into a continuous shell.

The fabrication of silver nanoshells has proven more difficult than the fabrication of gold nanoshells. Typically, it involves activation of the substrate surface by "seeds" of another metal, such as palladium or gold [32]. Dong et al. [33] reported the fabrication of nanoshells composed of close-packed silver nanocrystals on polystyrene spheres, by direct electrostatic attractions at appropriate pH. Song et al. [34] reported a facile wet-chemical approach for depositing silver nanoparticles on poly-(styrene-acrylic acid) (PSA) latex spheres. Mayer et al. [35] described several in situ chemical reduction methods to deposit silver layers on polystyrene (PS) latex spheres. Schueler et al. [36] reported deposition of silver onto PMMA latex particles via thermal evaporation techniques. More recently, Zhang et al. and Zhan et al. [28,37] prepared a complete metal (Ag or Au) shell with controlled thickness on polystyrene (PS) colloids by using the solvent-assisted route, and formed a complete silver shell. However, none of these reports have shown a systematic plasmon resonance tuning across the visible and infrared range of

the electromagnetic spectrum, upon depositing silver onto the polymer core.

Here, we report fabrication and characterization of silver and gold nanoshells on polystyrene (PS) spheres of different diameters, ranging from 188 to 543 nm. Our approach is to first functionalize the carboxylate-terminated polystyrene spheres with 2-aminoethanethiol hydrochloride (AET) to obtain thiol-terminated microspheres and then attach a partial layer of the gold nanoparticles that can be further grown in the presence of excess metal ions (silver or gold) to render a complete shell. We find that by varying the absolute shell thickness of the silver or gold on the polystyrene spheres, one can tune the peak of the surface plasmon absorbance band from the visible to the near-infrared (~500–940 nm). We also present the results of deposition of silver shells directly on ~12 nm gold nanoparticles that are not attached to a polystyrene sphere. These gold–silver core–shell structures are found to agglomerate into necklace-like chain aggregates and these aggregates also show systematic variation of the SPR peak across the visible spectrum.

## 2. Experimental section

2.1. Materials

A series of carboxylate-modified polystyrene particles (188, 296, and 543 nm, 10 wt% in water) were purchased from Seradyn Optilink^{TM}. HPLC water, 2-aminoethanethiol hydrochloride ($NH_2CH_2CH_2SH \cdot HCl$, AET, 98%), tetrakis(hydroxymethyl)phosphonium chloride (THPC, 80% solution in water), and hydrogen tetrachloroaurate(III) trihydrate ($HAuCl_4 \cdot 3H_2O$) were purchased from Aldrich. N-ethyl-N-(3-dimethylaminopropyl)carbodiimide hydrochloride ($C_8H_7N_3 \cdot HCl$, EDAC) and 2-(N-morpholino)ethanesulfonic acid (MES, >99.5%) were purchased from Sigma. Sodium citrate, formaldehyde (37% solution in water/methanol) and ammonium hydroxide (28–30%) were purchased from J.T. Baker. Silver nitrate ($AgNO_3$) was purchased from Alfa Aesar. All chemicals were used as received. HPLC-grade water was used at every stage of reaction and washing.

2.2. Synthesis

An outline of the method of preparation of silver and gold nanoshells is presented in Scheme 1. The detailed steps are as follows:

2.2.1. Functionalization of the surface of polystyrene particles with AET

AET can be covalently bonded to the surface of carboxylate-modified polystyrene particles. The carboxyl groups on the surface of polystyrene particles were activated by N-ethyl-N-(3-dimethylaminopropyl)carbodiimide hydrochloride (EDAC), then reacted with free amino groups of AET molecules to form amide bonds. To do this, 0.4 ml of MES stock buffer solution (500 mM, pH 6.1) was added to 0.4 g of the carboxylate-modified polystyrene dispersion with vigorous stirring. 3.2 ml of HPLC water was added to bring the total volume to 4 ml. Next,
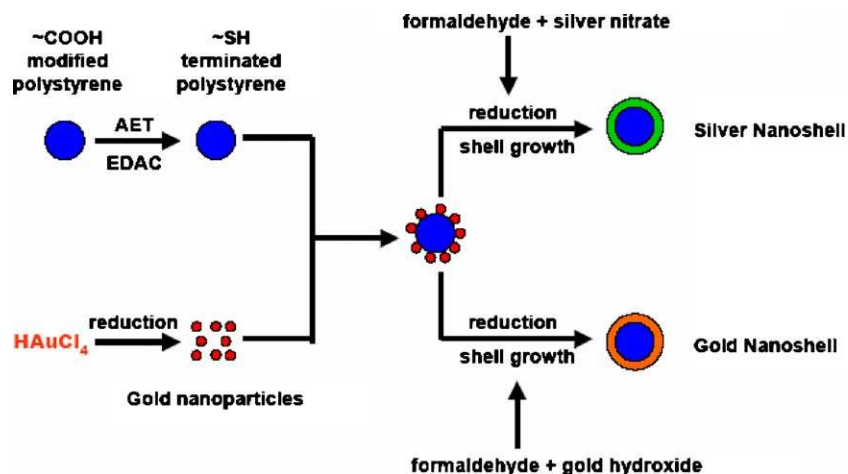
Scheme 1. Schematic illustration of the synthesis of gold and silver nanoshells on polystyrene beads.

3.5 ml of 52 mM EDAC solution was added into the mixture. After 30 min of stirring, 15 mg of AET in 0.5 ml of HPLC water was added. The mixture was stirred for 3–4 h, then centrifuged at 10,000 rpm (8736 × g) for 10 min to remove excess EDAC and AET from the AET-functionalized polystyrene particles. This step was repeated at least three times. The white precipitate was redispersed in 20 ml HPLC water.

2.2.2. Preparation of colloidal gold nanoparticles

The synthesis of gold colloids typically involves the reduction of gold salts in the presence of surfactants or stabilizers. In this study, two types of colloidal gold nanoparticles were prepared by reduction of chloroauric acid, using sodium citrate or tetrakis(hydroxymethyl)phosphonium chloride (THPC), respectively, as the reducing agent. Particles resulting from these two preparations are hereafter called citrate-gold and THPC-gold, respectively. The preparation of citrate-gold followed the method of Weiser [38,39]. In brief, 10 ml of HAuCl$_4$ (5 mM) solution was added to a flask containing 85 ml of boiling HPLC water, and the mixture was allowed to return to a boil. Then, a freshly prepared sodium citrate solution (5 ml, 0.03 M) was added to the mixture. A few minutes later, the solution changed from colorless to deep wine-red. The resulting red sol contained citrate-gold nanoparticles approximately 12 nm in diameter. At this point, the heating was stopped and the mixture was allowed to cool overnight. For the preparation of THPC-gold nanoparticles, the method described by Pham et al. [24] was adopted. 0.5 ml of freshly prepared 1 M NaOH and 1 ml of THPC solution (prepared by adding 12 μl of 80% THPC in water to 1 ml of HPLC water) were added to a flask that contained 45 ml of HPLC water. The reaction mixture was stirred for 5 min and then 10 ml of 5 mM HAuCl$_4$ was added. The color of the mixture changed from yellow to dark brown, indicating the formation of THPC-gold nanoparticles. The reduction of chloroauric acid with tetrakis(hydroxymethyl)phosphonium chloride (THPC) results in relatively small gold nanoparticles, ∼2 nm in diameter, with a net negative interfacial charge. In the work described below, we used colloidal gold nanoparticles ∼2 nm (THPC-gold) or ∼12 nm (citrate-gold) in diameter that were routinely prepared by the procedures outlined above.

2.2.3. Attachment of gold nanoparticles to AET-functionalized polystyrene particles

To attach citrate-gold to AET-functionalized polystyrene particles, 5 ml of AET-functionalized polystyrene solution and 50 ml of citrate-gold solution were mixed with vigorous stirring that led to the attachment of citrate-gold nanoparticles to the thiol groups on the surface of the AET-modified polystyrene particles. To remove the remaining free gold nanoparticles from the mixture, the above solution was centrifuged at 10,000 rpm (8736 × g) for 10 min, the supernatant removed, and the reddish precipitate redispersed in 20 ml HPLC water. This centrifugation step was repeated several times. The solution was further filtered using an Isopore^{TM} polycarbonate membrane filter with a nominal pore diameter of 100 nm (for 188 nm PS) or 200 nm (for 296 and 543 nm PS). Finally, the Au/AET/polystyrene nanoparticles were redispersed in 50 ml of HPLC water. The citrate-gold-decorated polystyrene particles have relatively low colloidal stability. Precipitation occurs after several hours, but the precipitate can be redispersed by ultrasonication. Similarly, to attach THPC-gold to AET-functionalized polystyrene particles, 5 ml of AET-functionalized polystyrene solution and 12.5 ml of THPC-gold solution were mixed with vigorous stirring. The solution was stirred for at least 30 min. Excess free THPC-gold nanoparticles were removed in the same manner as described above for the citrate-gold-decorated polystyrene particles. Finally, the precipitate was redispersed in 50 ml of HPLC water. The THPC-gold-decorated polystyrene particles have relatively high colloidal stability compared to the citrate-gold-decorated polystyrene particles, and stayed well dispersed in water for more than 4 weeks.

2.2.4. Silver shell growth

Silver nanoshells were made following the method reported by Jackson et al. [40] for silver deposition onto gold-decorated silica microspheres, which is an adaptation of the Zsigmondy method [41] for gold-nucleated growth of metal colloids. In brief, the gold-decorated polystyrene particles were mixed with

a fresh 0.15 mM solution of silver nitrate ($AgNO_3$) and stirred vigorously. Then, 50 µl of 37% formaldehyde was added to the stirred mixture to begin the reduction of silver onto the gold-decorated polystyrene particles. This step was followed by the addition of ammonium hydroxide (typically 20–50 µl of 28–30% NH_4OH). Over the course of 30–60 s, the solution changed from colorless to light blue, which is evidence of shell formation. The addition of NH_4OH into the sample solution caused a rapid increase in the pH of the solution, which facilitated in the reduction of Ag^+ to Ag^0 that deposited onto the surface of the seed particles, forming silver nanoshells. The ratio of the volumes of the dispersion of gold-decorated polystyrene particles to the silver nitrate solution controlled the amount of silver available for deposition on the polystyrene surface.

The formation of silver nanoshells rather than free silver nanoparticles depends on maintaining conditions where particle growth is favorable, but new particle nucleation is not. We observed that shells did not readily form on the surface of PS when a strong reducing agent, such as sodium borohydride, was employed. In this case, the large driving force for silver reduction appears to lead to nucleation of free silver particles before the Ag^+ ions can diffuse to the gold-decorated PS surface. As a result, partially coated or uncoated polystyrene spheres were obtained. Therefore, a careful selection of the reducing agent is crucial for obtaining a continuous silver nanoshell formation. We followed the approach used by Jackson and Halas [40], using formaldehyde as the "slow" reducing agent to initiate silver ion reduction onto the gold seeds. Subsequent addition of NH_4OH then fully reduced the silver precursor onto the seeded PS spheres.

2.2.5. Gold shell growth

The THPC-gold-decorated polystyrene particles mentioned above were also used to synthesize gold nanoshells. The THPC-gold particles attached to the PS spheres were used as nucleation sites for the further reduction of gold, resulting in deposition of a thin layer of gold on the nanoparticle surface. To grow the gold shell on the gold-decorated PS spheres, a solution of gold hydroxide was prepared first [27]. In a reaction flask, 0.05 g potassium carbonate (K_2CO_3) was dissolved in 185 ml HPLC grade water. Then, the solution was stirred for 10 min. Next, 15 ml of 5 mM $HAuCl_4$ was added to the solution. The mixture was initially light yellow and slowly became colorless after 30 min, indicating the formation of gold hydroxide. The resulting solution was aged for 24 h in the dark before it was used. The gold-decorated polystyrene particles were mixed with gold hydroxide solution and then stirred gently. 50 µl of 37% formaldehyde was added to the stirring mixture to begin the reduction of gold on to the gold-decorated polystyrene particles. This step was followed by the addition of (28–30% NH_4OH) ammonium hydroxide to adjust the pH of the solution to be slightly basic [42]. This typically required 20–50 µl of NH_4OH solution. The solution was gently stirred for approximately 9 h. During this time, the solution changed from colorless to light blue, which is an indication of shell formation. The solution was then allowed to stand for 1 h. By varying the volume ratio of gold hydroxide to PS particle solutions, the thickness of gold

nanoshell could be varied. To investigate the effect of the reducing agent on the gold nanoshell morphology and formation of free gold nanoparticles, other reducing agents such as sodium borohydride and hydroxylamine hydrochloride were also used to deposit gold from solution onto the THPC-gold-decorated PS (see Section 3).

2.3. Characterization methods

2.3.1. UV–vis absorbance

The absorption spectra were collected using a Shimadzu model 3101PC UV–vis-NIR scanning spectrophotometer, over wavelengths from 300 to 1300 nm. The samples were measured against water as reference. All samples were dispersed in water and loaded into a quartz cell for measurement.

2.3.2. Transmission electron microscopy (TEM)

Transmission electron microscopy (TEM) images were obtained using a JEOL model JEM-100CX microscope at an acceleration voltage of 80 kV. The specimens were prepared by drop-coating the sample dispersion onto an amorphous carbon coated 300 mesh copper grid, which was placed on filter paper to absorb excess solvent.

2.3.3. Scanning electron microscopy (SEM)

Scanning electron microscopy (SEM) images were obtained using a Hitachi S4000 field emission miscroscope at an acceleration voltage of 25 kV.

3. Results and discussion

3.1. Polystyrene size effects on the surface coverage of gold nanoparticles

The strategy used to prepare silver and gold nanoshells is illustrated in Scheme 1 and described in the previous section. Fig. 1 shows TEM images of 188, 296, and 543 nm polystyrene spheres after surface modification and attachment of ~2 nm diameter THPC-gold and ~12 nm diameter citrate-gold nanoparticles. Our previous studies have shown that a coverage of up to about 50% could be achieved by this method for 296 nm PS spheres, depending on the size of the gold nanoparticles [31]. The images in Fig. 1 show that, at least for the citrate-gold, as the size of the PS increases, so does the coverage of the Au nanoparticles. In these experiments, we used a fixed mass ratio of gold nanoparticles to polystyrene, so that number of available gold nanoparticles per PS surface area decreased with decreasing particle diameter (total PS surface area was inversely proportional to diameter). However, we always used an excess of gold nanoparticles, and the binding of the gold nanoparticles to the PS was irreversible. Therefore, the changes in particle binding density are not due to changes in the ratio of gold nanoparticle to PS surface area. This suggests that the curvature of the PS surface has an influence on the binding of the Au particles to the PS surface. As the surface curvature decreased (diameter increased), the particle coverage increased.
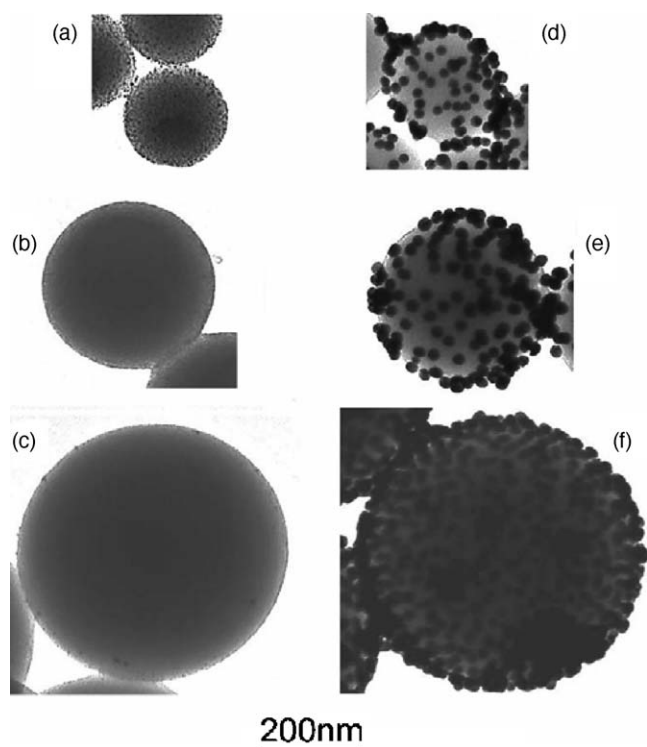
Fig. 1. TEM images of 188, 296, and 543 nm polystyrene spheres with (a–c) ∼2 nm THPC-gold and (d–f) ∼12 nm citrate-gold attached to their surface. As the size of the polystyrene core increased, the coverage of citrate-gold also increased.

3.2. Morphology of silver nanoshells

The silver nanoshells were grown by the reduction of silver nitrate onto the gold nanoparticles, which serve as nucleation sites. Depending on the extent of coverage of silver on these particles, pink-red, light blue or purple-blue solutions were observed for all PS sizes. The silver-coated nanoparticles have moderate colloidal stability, and precipitated noticeably after about a day. The precipitate could be redispersed by ultrasonication.

The silver nanoshells formed using THPC-gold-decorated polystyrene particles have a relatively smooth surface, but are less smooth than gold nanoshells prepared by the same procedure using THPC-gold seeds [31]. Figs. 2–4 show representative sequences of TEM images of THPC-gold-decorated 188, 296, and 543 nm PS nanoparticles, after reduction of increasing amounts of silver onto them. This illustrates the progressive metal nanoshell growth that occurs during reduction. Initially, a small fraction of the gold seed particles increases in size as the silver reduction progresses. Then the growing seeds coalesce on the nanoparticle surface. Finally, a continuous silver nanoshell is formed on the surfaces of the polystyrene cores. In TEM images of larger numbers of nanoshells we observed that all particles had complete silver shells of nearly uniform apparent thickness.

The formation of silver nanoshells using citrate-gold-decorated PS is similar to that using THPC-gold-decorated PS, except that the gold seeds are about six times larger in diameter (∼200 times larger in volume). This allows us to investigate
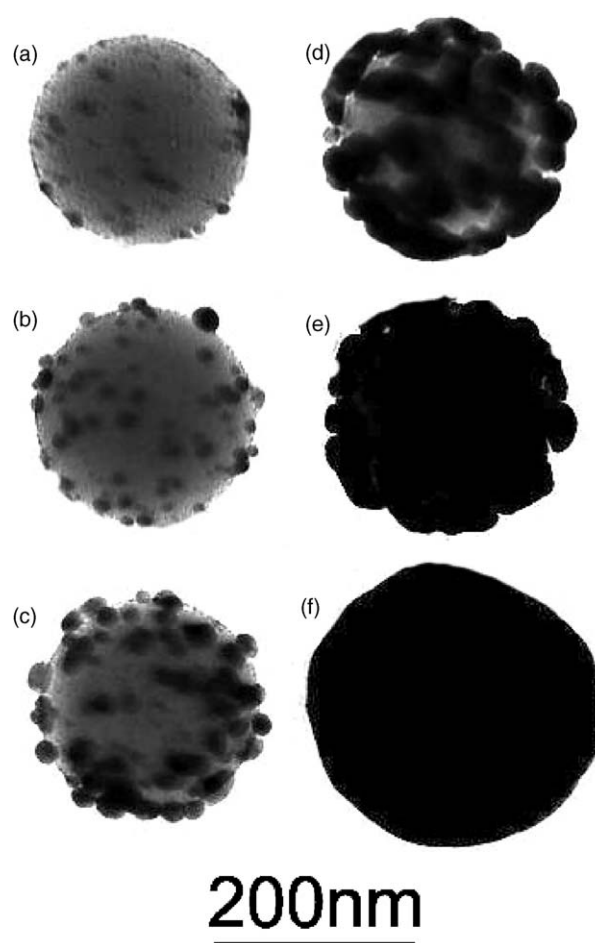

Fig. 2. TEM images of silver nanoshell growth on 188 nm polystyrene particles seeded with THPC-gold: (a–e) gradual growth and coalescence of silver particles on the polystyrene particle surface; and (f) a complete silver nanoshell.

the effect of seed size on morphology of the resulting silver nanoshells. Representative TEM images of silver nanoshells formed on 188 and 296 nm citrate-gold-decorated PS nanoparticles are presented in Fig. 5. The silver nanoshells formed in this case have relatively rough surfaces, due to the relatively large size of the citrate-gold nanoparticles used as seeds on the PS surface. These nanoshells have greater tendency to aggregate and precipitate than the corresponding shells grown with THPC-gold seeds. In a previous study, we used citrate-gold-decorated 296 nm PS spheres to obtain gold nanoshells. Many large gold particles (∼120 nm) were simultaneously formed in the process of growing a complete gold shell on these particles [31]. However, this phenomenon was not observed upon reducing silver onto the citrate-gold seeds. As was the case for the formation of gold nanoshells on polystyrene, the shells formed using citrate-gold seeds were rougher than those formed using THPC-gold seeds. However, the difference was less pronounced for silver shells than for gold shells because the THPC-gold-seeded silver shells were somewhat rougher than the THPC-gold-seeded gold shells prepared previously. Rough shells like those shown in Fig. 5 may be of particular interest for use in surface-enhanced Raman spectroscopy.
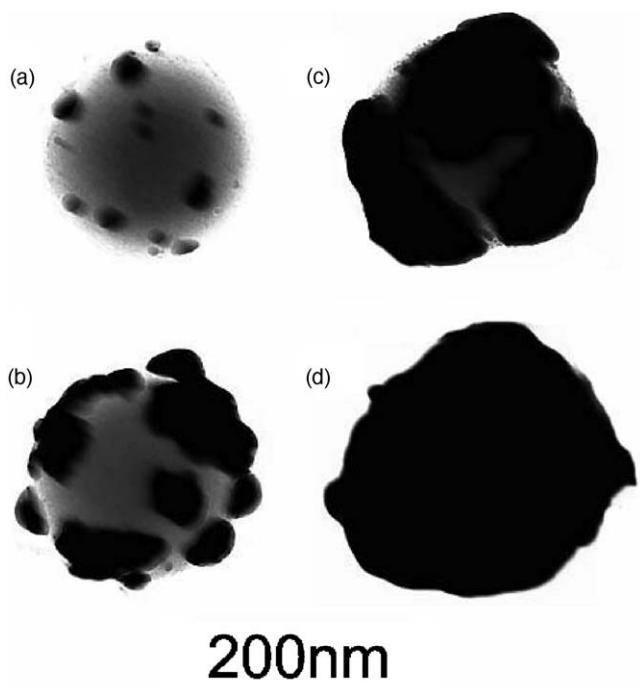
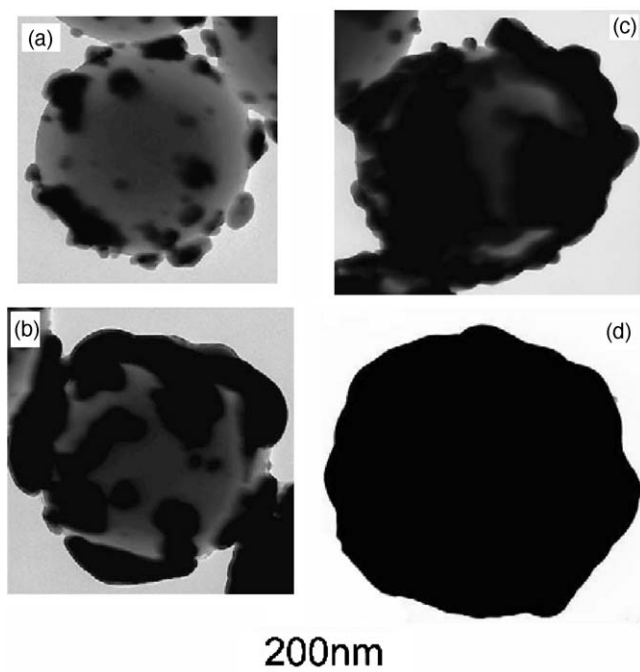Fig. 3. TEM images of silver nanoshell growth on 296 nm polystyrene particles seeded with THPC-gold: (a–c) gradual growth and coalescence of silver particles on the polystyrene particle surface; and (d) a complete silver nanoshell.

Observation of the gradual growth of silver particles on the THPC-gold-decorated polystyrene particles showed that only a small fraction of the THPC-gold particles grew. However, nearly all of the citrate-gold seed particles grew simultaneously to form the shell on the surface of the polystyrene sphere. Most

Fig. 4. TEM images of silver nanoshell growth on 543 nm polystyrene particles seeded with THPC-gold: (a)–(c) gradual growth and coalescence of silver particles on the polystyrene particle surface; and (d) a complete silver nanoshell.
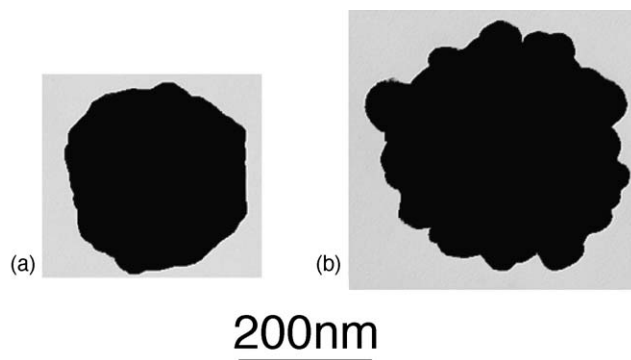

Fig. 5. TEM images of completed silver nanoshells formed using (a) 188 nm and (b) 296 nm polystyrene particles decorated with citrate-gold.

of the ~2 nm THPC-gold particles did not effectively seed silver growth. Those that did grow may have been agglomerates of a few smaller seeds or they may have undergone a nucleation-like event in which enough silver deposited to exceed the critical nucleus size for particle growth. This suggests that there is a critical nucleus size for the growth of silver particles on gold seeds that is larger than ~2 nm but smaller than ~12 nm. This limits the smoothness of the shells that can be formed in this approach, since it limits the maximum density of effective seed particles.

3.3. Morphology of gold nanoshells

The 188 and 543 nm polystyrene spheres decorated with ~2 nm diameter THPC-gold nanoparticles were also used to synthesize gold nanoshells. In this study, three techniques previously reported for fabricating gold nanoshells on silica microspheres were adapted to produce gold nanoshells on polystyrene spheres. The first method followed a deposition protocol previously reported by Oldenburg et al. [27] in which varying amounts of gold hydroxide were added to THPC-gold-decorated polystyrene particles, then 20 μl of sodium borohydride (0.033 M in water) was added with vigorous stirring. The color of the solution instantaneously changed from colorless to red or pinkish, indicating the formation of gold colloids. It appeared that sodium borohydride, a relatively strong reducing agent, induced formation of gold nanoparticles on a time scale too short for significant gold deposition onto the gold-decorated PS spheres. As a result, partially coated or uncoated polystyrene spheres were obtained, along with large quantities of free gold nanoparticles. The second method was based on the approach reported by Graf et al. [43], in which THPC-gold-decorated polystyrene spheres were mixed with different amounts of gold hydroxide under vigorous stirring, then 10 ml of hydroxylamine hydrochloride (1.87 mM in water) was added drop-wise into the mixture. This resulted in a black precipitate and a purple-blue solution, from the formation of both free gold and nanoshells in the solution as previously reported for 296 nm diameter cores [31]. Repeated centrifugation and washing was required to separate gold nanoshells from the free gold. Gold nanoshells as well as large gold particles and agglomerates were formed as shown in Fig. 6. We observed that these newly formed gold
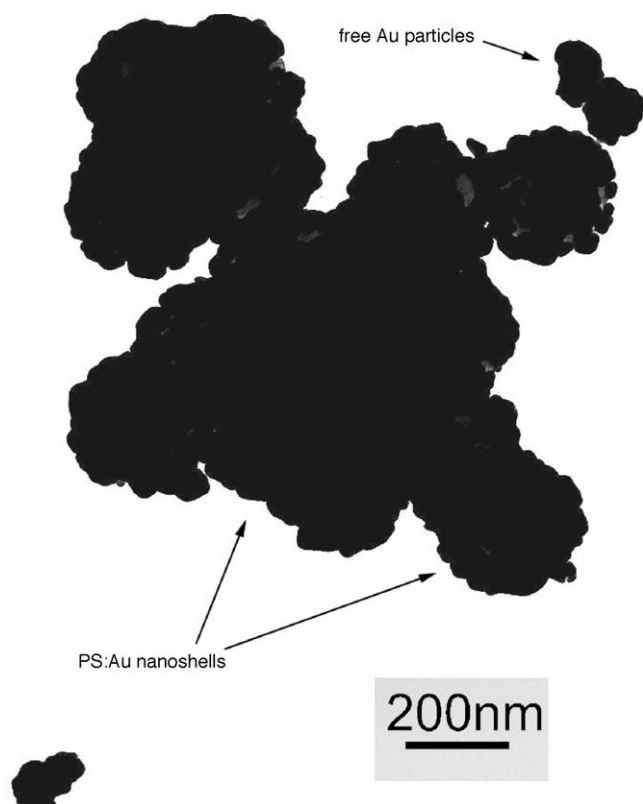
Fig. 6. TEM image of agglomerates of free gold nanoparticles and nanoshells produced using hydroxylamine hydrochloride as the reducing agent.
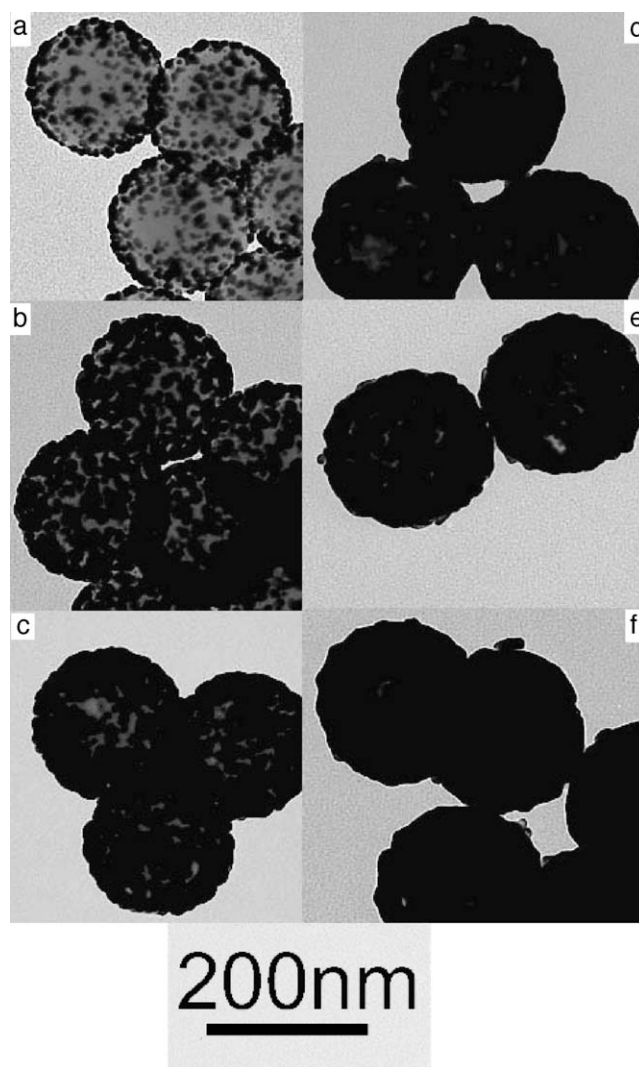

Fig. 7. TEM images of nanoshells grown on 188 nm gold-decorated polystyrene spheres using formaldehyde as the reducing agent: (a–e) gradual growth and coelesence of gold seed particles on the polystyrene particle surface; and (f) complete gold nanoshell.

particles often attached to the surface of gold nanoshells. The resulting 'clumps' could not easily be removed from the gold nanoshells.

The gold nanoshells prepared by the above methods did not provide the desired thin, uniform coating of the polystyrene spheres. To achieve this, it is important that all small gold nanoparticles grow evenly, so that, after the particles have grown to a few nanometers, all gold particles will coalescence and the resulting gold shell has a uniform thickness. Formation of thinner gold shells will, for a given core size, also result in a larger red shift of the surface plasmon resonance absorbance. In addition, the formation of free gold particles in solution should be prevented or minimized to reduce the amount of post-synthetic washing required. This can better be accomplished using a modification of the method reported by Lim et al. [42]. In this method, formaldehyde serves as a "slow" reducing agent to reduce gold ions onto the gold-decorated microspheres. Shell deposition occurred as the mixtures were stirred gently over 9 h. The gold nanoshells were obtained directly without centrifugation. No free gold nanoparticles were formed using this method. The gold nanoshells formed by this method have a somewhat rough surface.

Figs. 7 and 8 show a sequence of TEM images of 188 and 543 nm PS spheres after reduction of increasing amounts of gold onto the THPC-gold-decorated spheres, illustrating the progressive growth of metal nanoshell during reduction. At low volume ratio of gold hydroxide to polystyrene particle solutions, gold nanoparticles with a diameter of ~5–9 nm were distributed

uniformly on the polystyrene surface (Fig. 7a). Although the gold particles were attached and grew with the reduction process, complete gold shells were not obtained simply because not enough gold was present. For higher volume ratios of gold
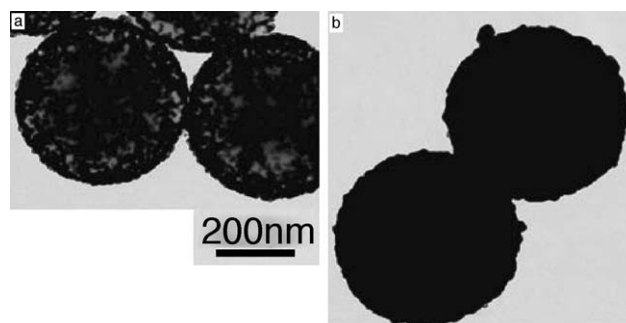

Fig. 8. TEM images of (a) partial and (b) complete gold nanoshells grown on THPC-gold-decorated 543 nm polystyrene spheres using formaldehyde as the reducing agent.
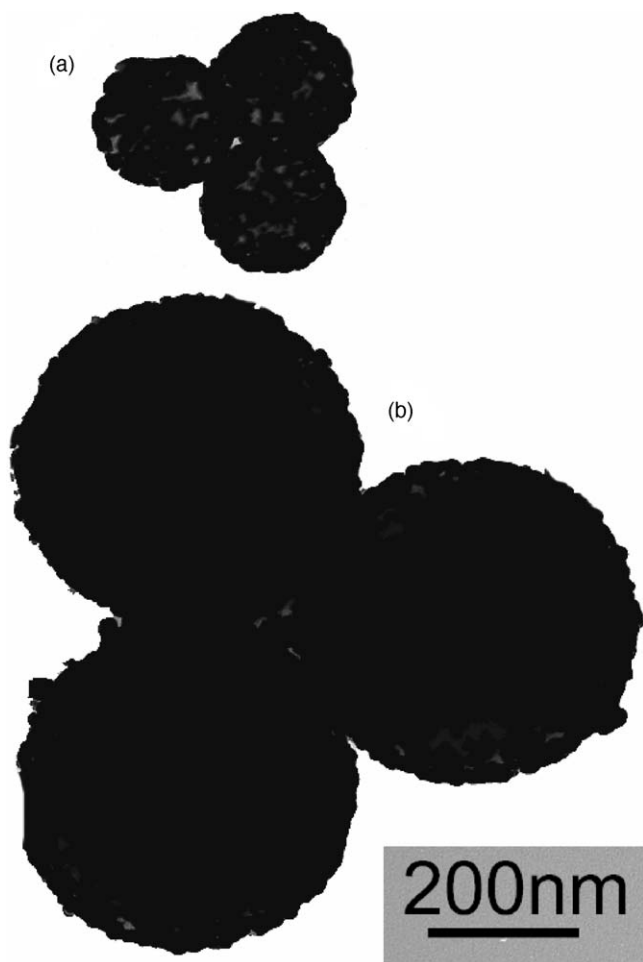
Fig. 9. TEM images of polystyrene spheres with partial gold coverage on their surface. The gold nanoshells often self-assemble into trimers with equilateral triangle geometry as shown here.

hydroxide to polystyrene particles solution, a complete gold nanoshell was formed as shown in Figs. 7f and 8b. In this case, the gold seeds began to coalesce on the surface of the polystyrene spheres, until a continuous gold nanoshell was formed. Overall, the surface of the gold nanoshell obtained in this method was rough as shown in Fig. 8f. Depending on the coverage of gold on these particles, light blue or purple-blue solutions were observed. The gold-coated nanoparticles have a moderate colloidal stability, with significant precipitation occurring on a time scale of 1 day. The precipitate could be redispersed in water by ultrasonication. The neat (uncoated) monodispersed polystyrene spheres readily self-assemble into an ordered assembly (two- or three-dimensional). As the adsorbed gold particles render the surface somewhat rough, the long-range order breaks down and mostly isolated particles or their dimers or trimers are observed, rather than larger ordered clusters (see TEM image in Fig. 9) [31]. Fig. 10 displays a TEM image of a larger quantity of partially covered spheres to indicate the degree of sphere-to-sphere uniformity of coverage at this point of transition from partial to complete shells. The coverage remained similar at different spots on the TEM grid.
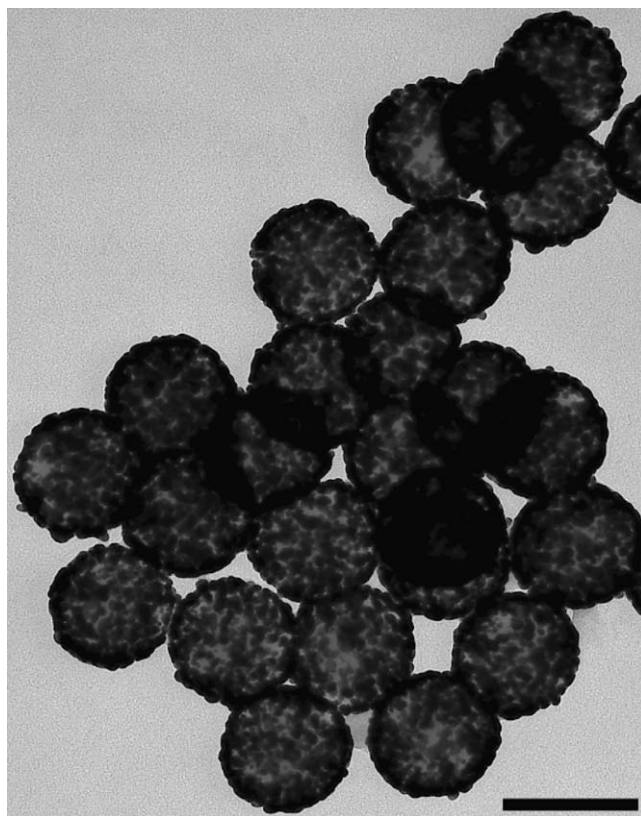

Fig. 10. TEM image demonstrating the uniformity of partially gold coverage on 188 nm polystyrene spheres. The scale bar is 200 nm.

3.4. Surface plasmon resonance absorbance of silver nanoshells

Deposition of silver onto the gold-seeded PS spheres leads to a shift in the SPR absorption. Extinction spectra of THPC-gold-decorated and citrate-gold-decorated PS spheres, with increasing silver nitrate to PS concentration ratios, illustrate this for a series of sizes of PS spheres. For free THPC-gold, no SPR peaks were observed (see Fig. 11). This is consistent with many literature reports that there is no SPR feature for such small Au particles. On the other hand, citrate-gold and silver nanoparticles have sharp SPR peaks at 520 and 400 nm, respectively (see Fig. 11). As the coverage of silver on THPC-gold-seeded PS increased, the SPR peak became more prominent and red shifted up to a maximum of 824 nm for 188 nm diameter PS
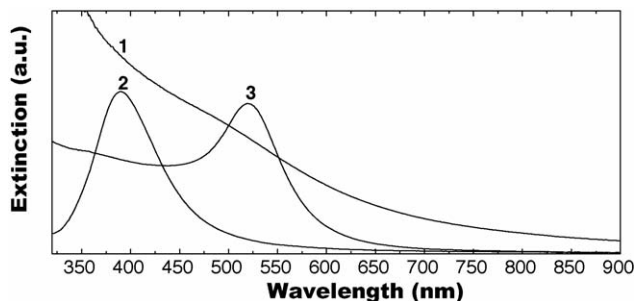

Fig. 11. Absorption spectra for (1) THPC-gold; (2) silver; and (3) citrate-gold nanoparticles.
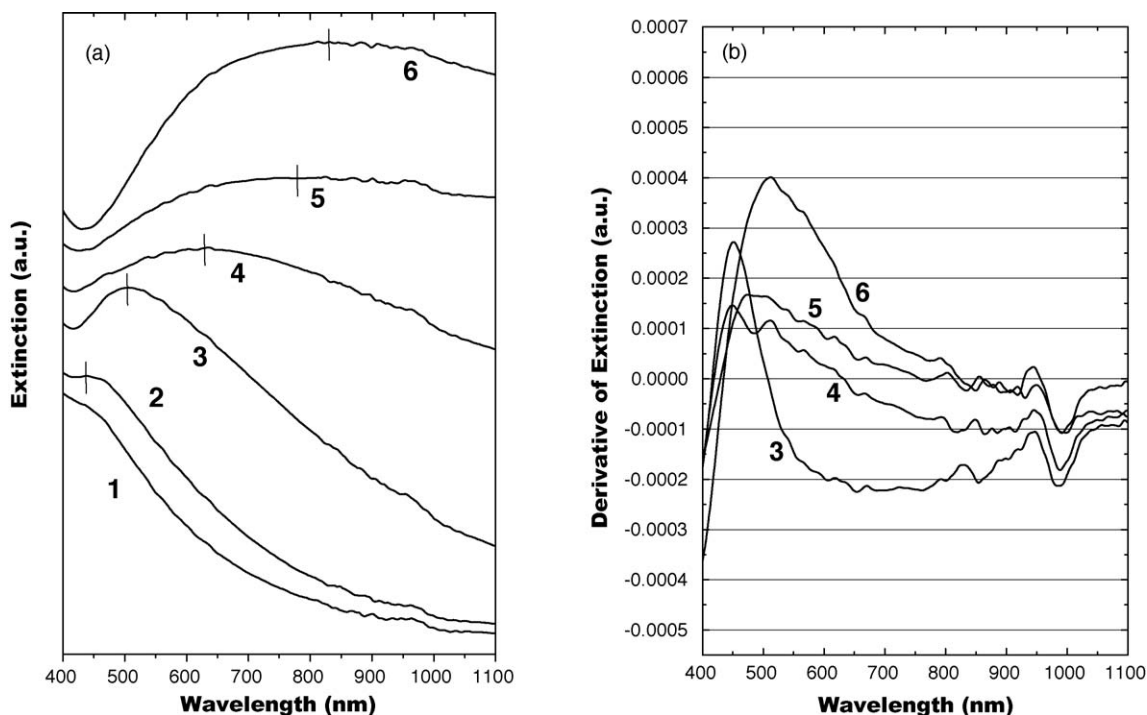
Fig. 12. (a) Absorption spectra of THPC-gold-decorated 188 nm polystyrene spheres with different coverage of silver on their surface resulting from different silver to PS ratios; and (b) the same data differentiated. Curves 3 through 6 cross zero at 507, 633, 759, and 824 nm. Curves 1 through 6 follow the evolution of the optical absorption as coalescence of the silver layer progresses and correspond to images (a) through (e) in Fig. 2.

cores, as shown in Fig. 12. A similar red shift of the SPR peak was observed for 296 and 543 nm sized PS cores, as shown in Figs. 13 and 14, respectively. This is accompanied by a substantial broadening of the SPR peak. Such systematic red shift is consistent with literature reports for gold and silver nanoshells, prepared by different procedures on silica microspheres [27,40]. Due to the broad nature of the peaks, the position of the extinction maximum in each case is more easily determined by examin-
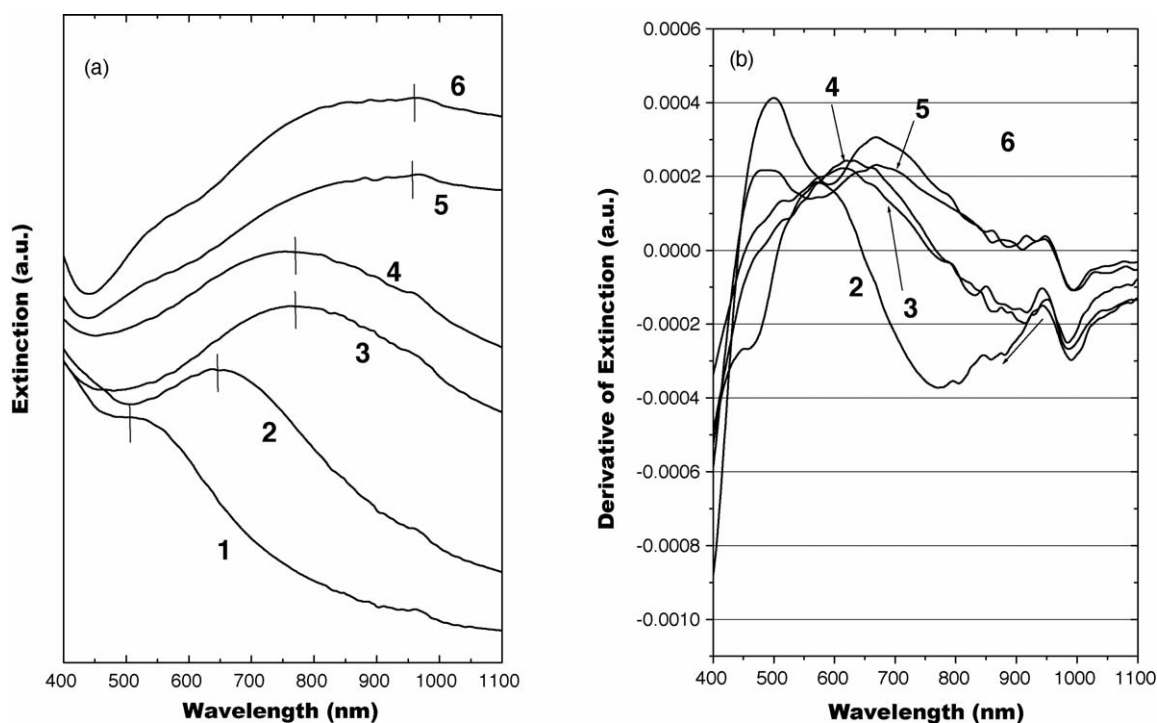

Fig. 13. (a) Absorption spectra of THPC-gold-decorated 296 nm polystyrene spheres with different coverage of silver on the surface resulting from different silver to PS ratios; and (b) the same data differentiated. Curves 2 through 6 cross zero at 645, 767, 757, 963, and 961 nm.
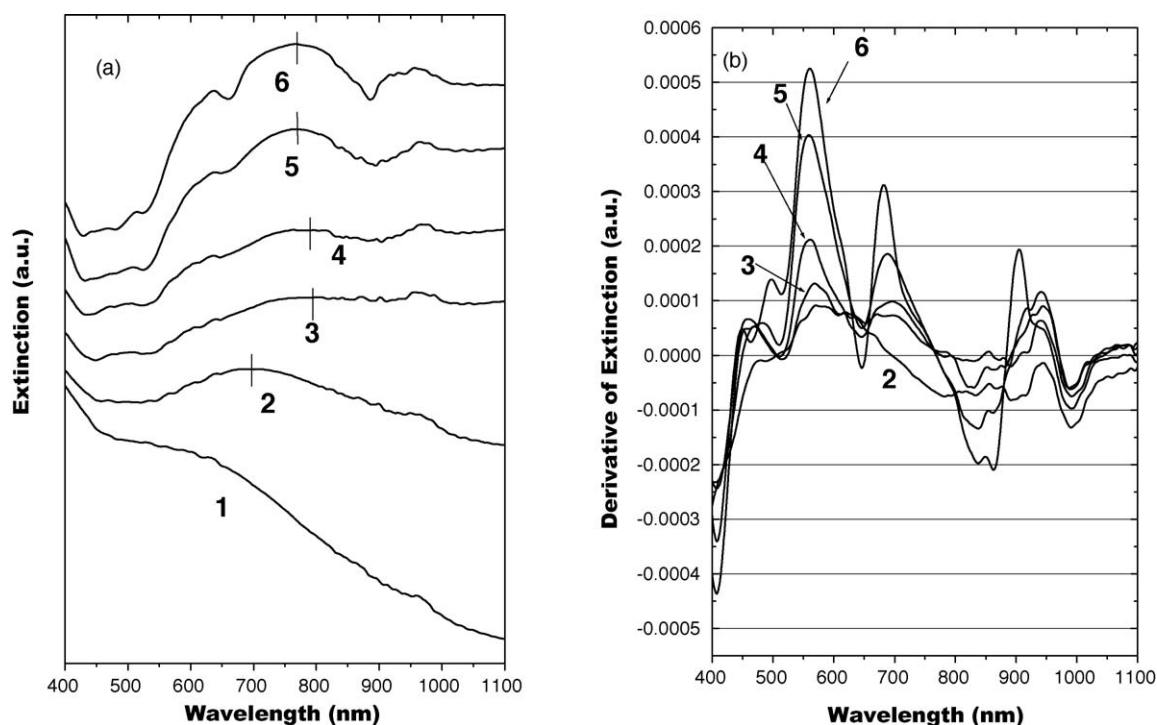
Fig. 14. (a) Absorption spectra of THPC-gold-decorated 543 nm polystyrene spheres with different coverage of silver on the surface resulting from different silver to PS ratios; and (b) the same data differentiated. Curves 2 through 6 cross zero at 696, 792, 777, 769, and 768 nm.

ing the derivative (slope) of the extinction spectrum where the first crossover point of the first differential is taken as the maximum of the curve. Once the PS surface is completely covered with silver, forming a continuous shell, no further red shift is observed.

The extinction spectra of 188 nm diameter citrate-gold-decorated PS spheres are presented in Fig. 15, as a function of the silver nitrate to PS ratio. At relatively low silver nitrate concentration, one strong SPR peak is observed at ~520 nm, which is attributed to the 12 nm citrate-gold bound to the surface of PS.
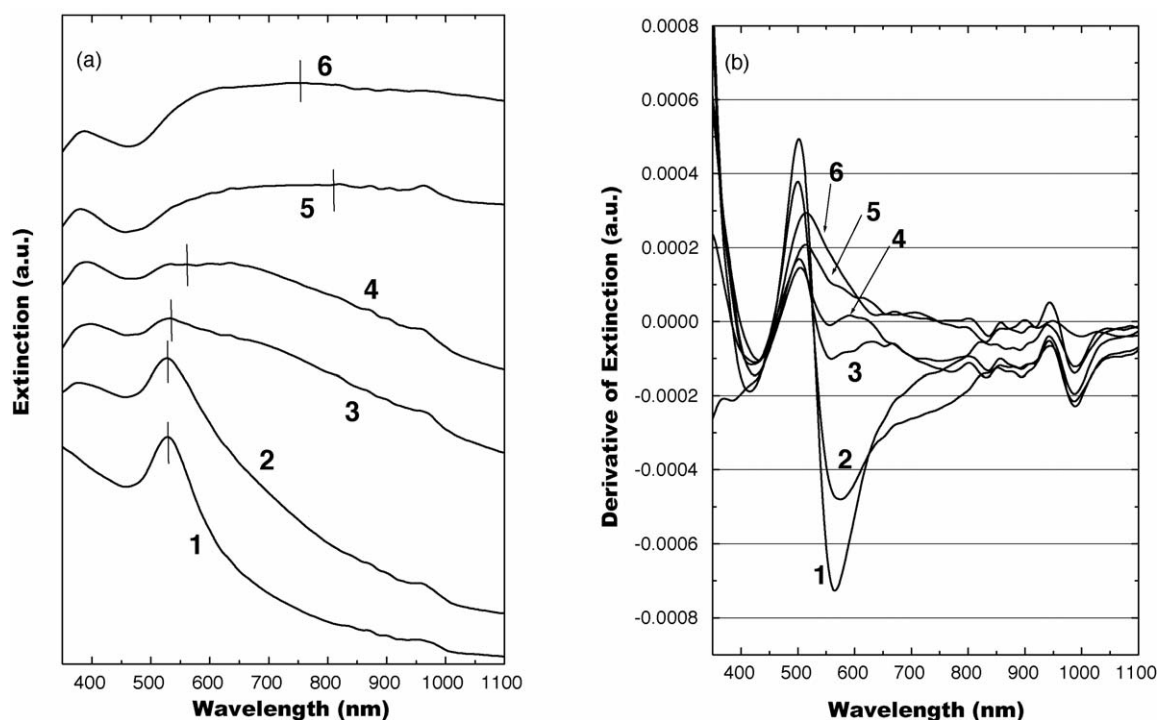

Fig. 15. (a) Absorption spectra of citrate-gold-decorated 188 nm polystyrene spheres with increasing coverage of silver on the surface resulting from increasing silver to PS ratio; and (b) the same data differentiated. Curves 3 through 6 cross zero at 527, 527, 532, 568, 812, and 748 nm.
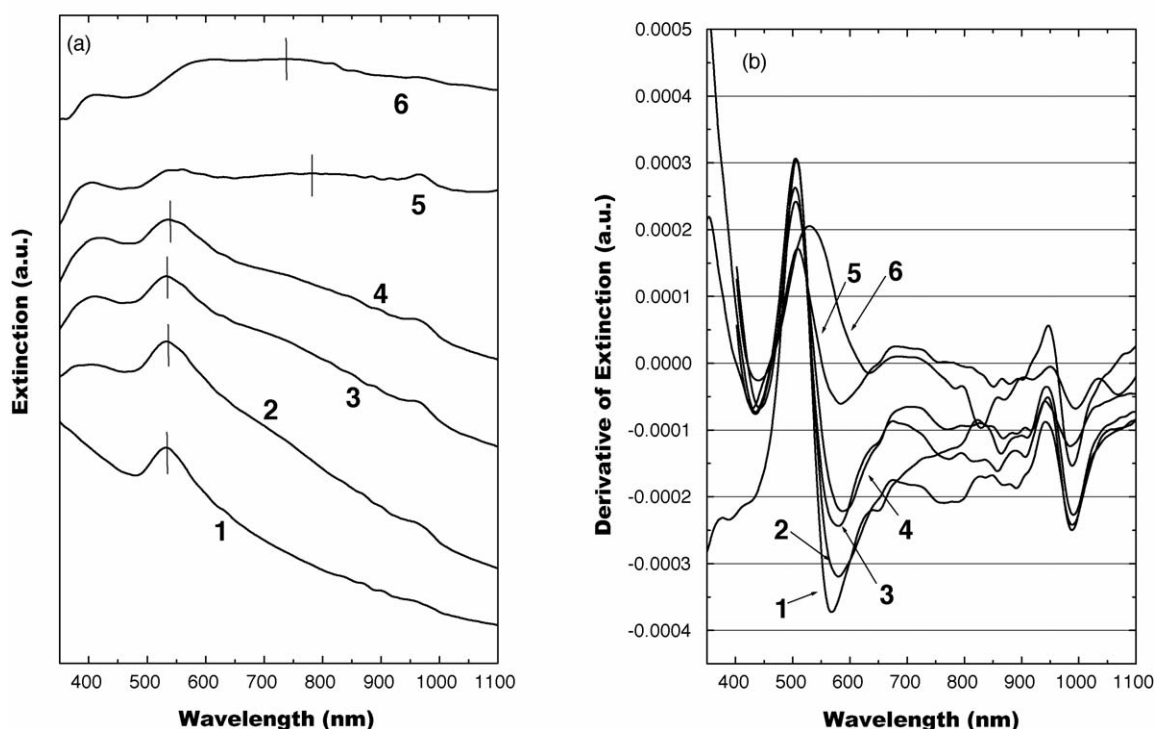
Fig. 16. (a) Absorption spectra of citrate-gold-decorated 296 nm polystyrene spheres with increasing coverage of silver on the surface resulting from increasing silver to PS ratio; and (b) the same data differentiated. Curves 3 through 6 cross zero at 532, 534, 534, 539, 784, and 735 nm.

Upon increasing the ratio of silver nitrate to PS, the prominent peak at 520 nm broadens and red shifts. Simultaneously, a SPR peak at ∼380 nm begins to develop. Similar spectra for 296 nm diameter cores are shown in Fig. 16.

3.5. Silver nanoshells on free citrate-gold nanoparticles

For comparison to the silver shells seeded with gold nanoparticles, we also reduced silver onto free cirate gold nanoparticles to form gold core/silver shell nanoparticles. Somewhat surprisingly, we have found that upon reducing increasing amounts of silver nitrate onto the citrate-gold nanoparticles, the surface plasmon resonance absorption peak red shifted systematically from its initial position near 520 nm across the visible and into the near IR range (∼800 nm). While both the plasmonic properties of Au/Ag core/shell structures and alloy structures have been studied in the past, this dramatic red shift of the SPR absorbance has not previously been observed. It is, in fact, unexpected for simple gold core/silver shell particles. Sato et al. [44] reported the photochemical formation of Ag–Au composites using sodium alginate as a stabilizer, and observed "only gold and silver domains". Mulvaney et al. [45] reported the radiolytic formation of Ag core–Au shell structures. Treguer et al. [46] used γ-irradiation of a solution of gold and silver salts to obtain core–shell type structures at low radiation doses, and alloys at high doses. Hodak et al. [47] reported the preparation of the Au core–Ag shell and Ag core–Au shell particles, where the core metal was made first, and the ions of the shell metal were subsequently reduced onto the surface of the core particles by a radiolysis technique. Schatz and coworkers [48]

reported that the preparation of gold-core/silver-shell nanoparticles by using a 'seed colloid' technique, where the silver ions were deposited on 13 and 25 nm gold particles by citrate reduction. It was found that the Au–Ag core–shell particles exhibited a single plasmon band that is blue-shifted to ∼400 nm with increasing silver content and, conversely, the plasmon resonance for the Ag–Au core–shell particles red shifted to ∼520 nm with increasing Au content. This is also what is predicted by the Mie scattering theory. With the preparation methods used here, we observed a systematic shift of the SPR absorption, which was not seen in any of the previous studies. Depending on the amount of silver reduced onto the fixed amount of citrate-gold, light blue, purple, light-green, green and orange-yellow solutions were observed, as shown in Fig. 17. Here, it should be mentioned that the citrate-gold colloid is sensitive to the solvent environment, particularly the pH and ionic strength. We performed a substantial array of control experiments to confirm that the color change was not an artifact of changes in pH, ionic strength, or solution composition.[1]

Fig. 18 shows TEM images of the citrate-gold nanoparticles after reduction of silver onto them. In these images, the gold core has higher contrast than the silver shell and appears darker.

---

[1] In the control experiments, we added formaldehyde, silver nitrate and ammonium hydroxide solutions independently to citrate gold sol at volumes and concentrations identical to our actual experiments. There is an instant color change of citrate Au sol from wine-red to purple on adding ammonium hydroxide and no color change in other cases. However, when all the three reagents were added in sequence as explained in the text, there was a sequential systematic change of color as depicted in the Fig. 7.

Fig. 17. Gold core–silver shell particles that absorb various wavelengths of light (the eight vials on the right), compared to gold colloid (far left).

The TEM images show that the silver-coated gold nanoparticles have agglomerated into necklace-like chain aggregates. Some free gold core/silver shell nanoparticles were also observed.

Fig. 19 shows the extinction spectra of these solutions with increasing silver nitrate to citrate-gold volume ratios. The absorption feature at 520 nm is due to the plasmon resonance of the citrate-gold nanoparticles. Focusing only on the region from 350 to 600 nm, the change in plasmon resonance absorption is qualitatively similar to that observed in previous studies, with the 520 nm gold resonance rapidly decreasing in intensity and the silver resonance at 400 nm increasing in intensity as the amount of silver reduced onto the particles increases. However, in these experiments, a second plasmon resonance absorption at a longer wavelength also develops when silver is added. This is not expected for simple Au-core/Ag-shell structures. Rather, this absorption can probably be ascribed to a collective plasmon resonance of the necklace-like aggregates shown in Fig. 18. Especially for small amounts of silver addition, the spectrum is qualitatively similar to that of gold nanorods that exhibit a transverse plasmon resonance near 520 nm and a longitudinal resonance at longer wavelength [49]. For curves 2 through 6 in Fig. 19, this longer wavelength absorbance is stronger than the absorbance in the 400–520 nm range, and, therefore, this longer wavelength absorbance determines the appearance of the colloid, as shown in Fig. 17. As silver was reduced onto the gold nanoparticles, an absorption band peaking at ∼712 nm appeared. This red shifted to a maximum of ∼807 nm with increasing silver content. Upon further increasing the silver nitrate to the citrate-

gold volume ratio, a pronounced blue shift ensued. At the 1:5 citrate-gold to silver nitrate volume ratio (see curve 9 in Fig. 19), the spectrum was dominated by the strong broad peak at 404 nm and absorption at longer wavelengths was less prominent. This is the spectrum expected for a pure silver colloid or for gold-core silver shell structures for large silver shell thickness. It was interesting to find that upon reducing silver onto the surface of citrate-gold (∼12 nm in diameter), the SPR peak red shifts in a similar fashion as that of silver nanoshells on a polystyrene core. This appears to be the first observation of a systematic plasmon resonance shift for a bimetallic system, where the plasmon resonance of the nanostructure can be tuned to a specific wavelength across the visible to near-infrared range of the electromagnetic spectrum. The question that remains unanswered is why the random necklace-like aggregates would cause the plasmon band to red shift so systematically. Thomas et al. [50] reported a new paradigm for tuning the optical properties of gold nanorods by organizing them longitudinally using thioalkylcarboxylic acid-based bifunctional molecules. The authors observed that upon aligning the gold nanorods in a longitudinal fashion, the plasmon band red shifted. The origin of the red shifted band on these linearly assemblies of gold nanorods was explained by means of a dipolar interaction mechanism. We speculate that the red shift observed here arises from the alignment of gold nanoparticles as the silver shells partially fuse and form the necklace-like chain aggregates. However, further theoretical studies are needed to verify this. In any case, this method is simple and straightforward, and may serve as an alternative approach to obtaining nanostructures with useful plasmonic properties.
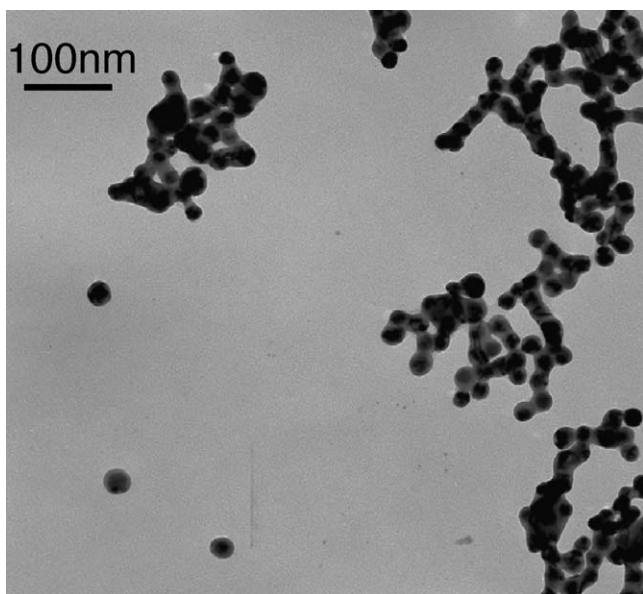
3.6. The surface plasmon resonance spectra of gold nanoshells

In the case of gold nanoshells, as the attached gold nanoparticles grew and merged, the surface plasmon resonance (SPR) systematically shifted, consistent with previous studies [31]. Figs. 20 and 21 show the extinction spectra of THPC-gold-decorated PS spheres after reduction of increasing amounts of gold hydroxide onto them. The UV–vis extinction spectra of THPC-gold-seeded 188 and 543 polystyrene spheres showed no absorption peaks. As the coverage of gold on THPC-gold-seeded PS increased, the SPR peak became more prominent and red shifted to a maximum of 932 and 931 nm for 188 and 543 nm PS, respectively. The observed spectra corresponded well to the TEM images shown above (Figs. 7 and 8), with higher coverage resulting in a larger red shift. The shift is accompanied by a substantial broadening of the SPR peak. Once the PS surface is completely covered with gold, forming a continuous shell, no further red shift is observed. The SPR peak then blue shifts with increasing shell thickness. When hydroxylamine hydrochloride

Fig. 18. TEM image of gold core/silver shell nanoparticles with both free particles and necklace-like chain aggregates.
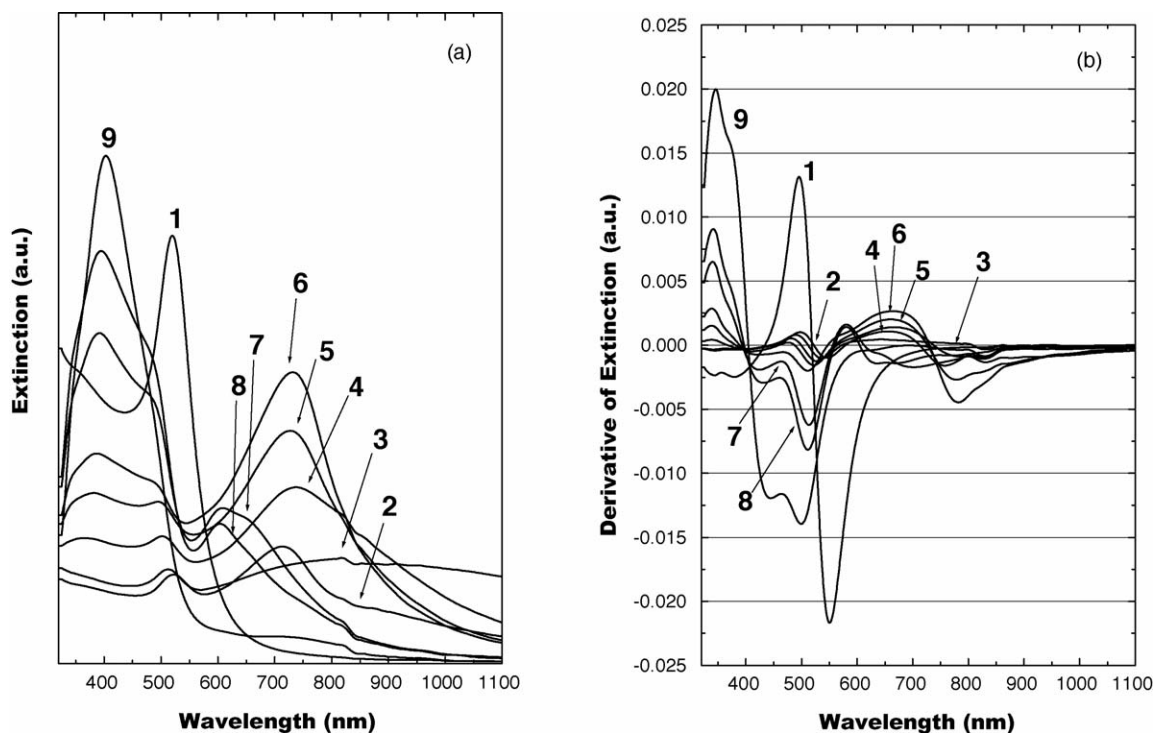
Fig. 19. (a) Absorption spectra for (1) pure citrate-gold and (2–9) citrate-gold spheres with different coverage of silver on the surface, resulting from different silver to citrate-gold ratios; and (b) the same data differentiated. Curves 1 through 9 cross zero at 518, 712, 807, 737, 726, 730, 612, 604, and 404 nm.
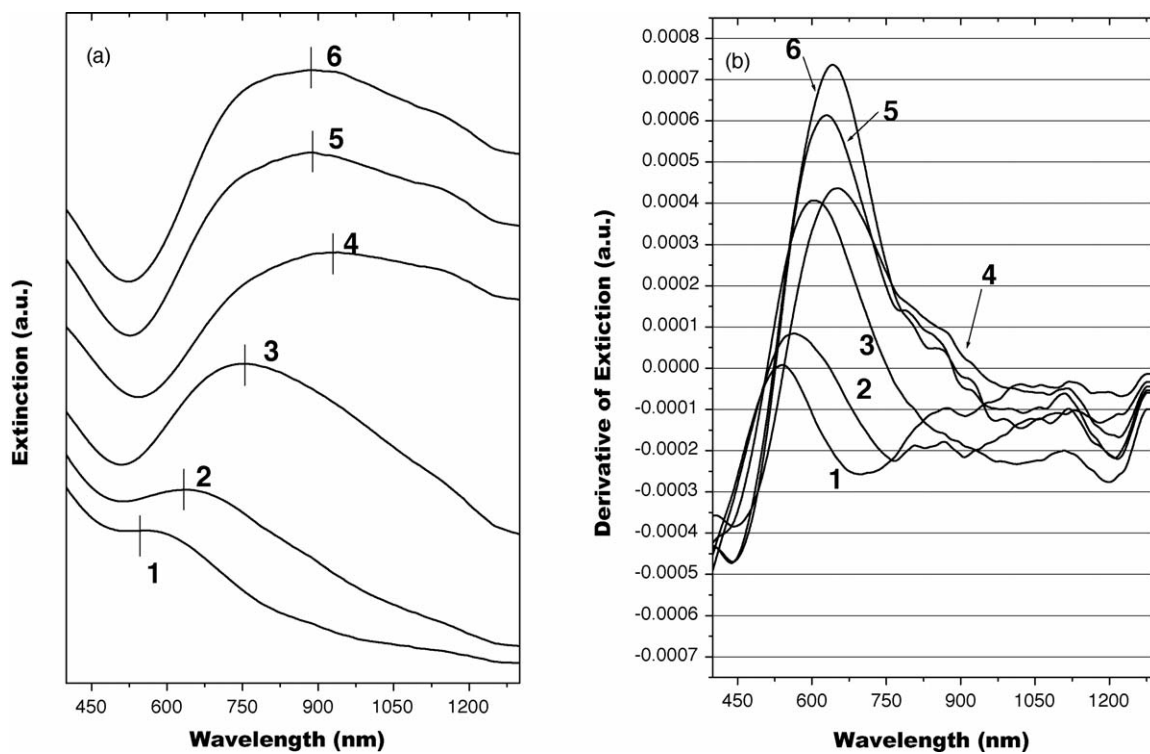

Fig. 20. (a) Absorption spectra of THPC-gold-decorated 188 nm polystyrene spheres with increasing coverage of gold on their surface; and (b) the same data differentiated. Curves 2 through 7 cross zero at 636, 753, 932, 884, and 888 nm. Curves 1 through 6 follow the evolution of the optical absorption as coalescence of the gold layer progresses and correspond to images (a) through (f) in Fig. 7.
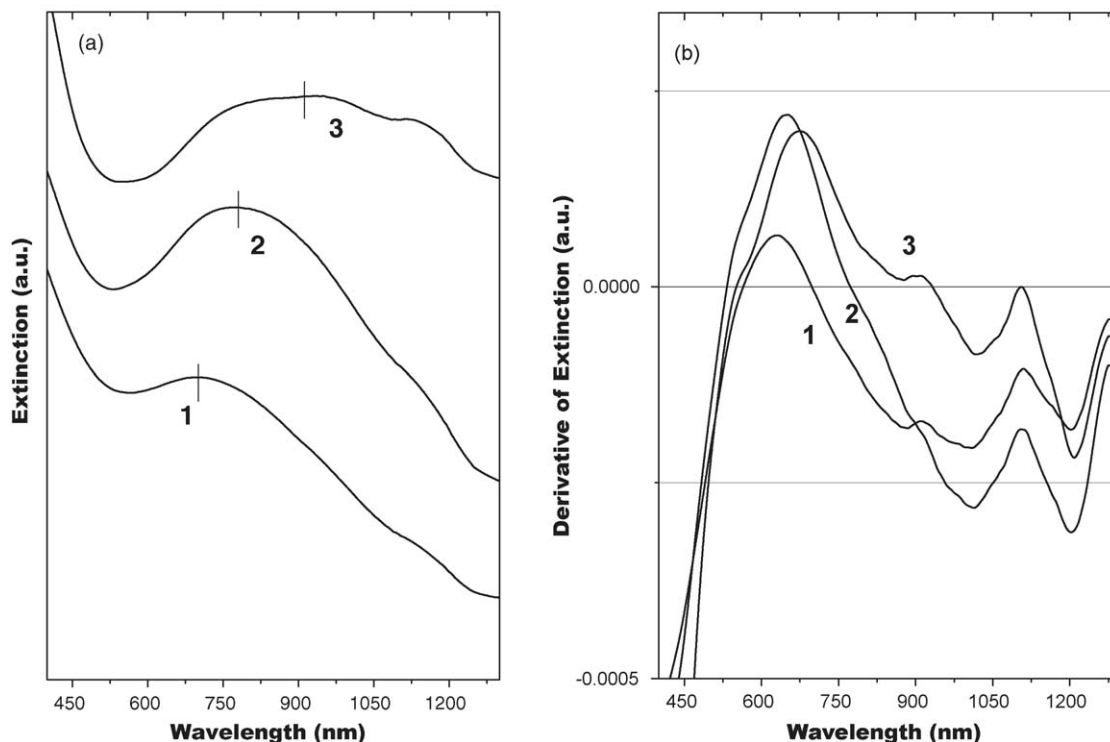
Fig. 21. (a) Absorption spectra of THPC-gold-decorated 543 nm polystyrene spheres with different coverage of gold on the surface resulting from different gold hydroxide to PS ratios; and (b) the same data differentiated. Curves 1 through 3 cross zero at 698, 772, and 931 nm.

was the reducing agent, both gold nanoparticles and nanoshells were formed, and the UV–vis extinction spectrum of this mixture showed a distinct peak between 520 and 600 nm, indicating that the SPR peak from the gold nanoshells was masked by the presence of the gold particles.

3.7. Comparison of experimental SPR absorption with extended Mie theory calculations

For complete continuous shells, the extinction spectra can be compared to those predicted by the extended Mie scattering theory for core–shell particles as developed by Aden and Kirker [51]. We have done so, using the formulation of the solution presented by Toon and Ackerman [52]. In computing the spectra, we have incorporated electron-interface scattering by using a size-dependent dielectric function for the gold shell, following the approach of Westcott et al. [53]. We have used a value of three for the parameter A in their model, which accounts for the angular nature of electron scattering, scattering at grain boundaries in the polycrystalline shell, and the shape of the core/shell and shell/surroundings interfaces. A significant complication for these polystyrene cores is the uncertainty in the core diameter. We observe substantial differences between the diameters stated by the manufacturer (which appear to be based on dynamic light scattering) and the diameters that we observe in TEM images of the bare polystyrene spheres. Unfortunately, the particles may shrink somewhat in the vacuum environment of the TEM, and therefore it is not clear that the diameters observed in TEM are those of the polystyrene cores in solution. For the shells on

188 nm nominal diameter cores, we have data for complete shells of both gold and silver. For these, a core diameter of 168 nm gave reasonable agreement between experimental and computed SPR absorption spectra. The diameters observed and used in calculations are shown in Table 1, and the experimental and computed spectra are shown in Fig. 22. For the nominally 543 nm cores, we obtain reasonable agreement between experimental and computed SPR absorption spectra using the core diameter of 428 nm that is observed in TEM.

3.8. Potential applications of silver nanoshells, gold nanoshells and gold core-silver shell NPs

Advanced materials derived from core–shell composite particles are of extensive scientific and technological interest because of their unique optical, electronic, and catalytic properties. Such silver-polystyrene composite particles with a core–shell structure are expected to have applications in surface-enhanced Raman scattering (SERS) and catalytic studies. SERS has been a subject of extensive studies. It is generally agreed that an important contribution to the SERS enhancement comes from the electromagnetic (EM) enhancement mechanism, in which plasmon excitation in the particle creates an enhanced electric-field near the particle, which in turn leads to enhanced Raman excitation and emission [27]. Furthermore, the SPR absorption of these composite particles could be tailored to the wavelength regions of 800–1300 nm by varying the core size and the shell thickness, which is the spectral region best suited for optical bioimaging, biosensing and thermal therapy applications

Table 1
Core and shell diameters from experiment and used in calculations

Experimental			Calculated	
Diameter of polystyrene particles[a] (nm)	Measured average diameter values from TEM[b] (nm)	Total average diameter of nanoshells (nm)	Diameter of polystyrene (nm)	Total diameter of nanoshells (nm)
Silver nanoshells				
188	142.9 ± 9.5	199.3 ± 15.2	168	199
Gold nanoshells				
188	142.9 ± 9.5	196.3 ± 6.0	168	196
188	142.9 ± 9.5	200.9 ± 7.0	168	201
543	428.6 ± 19.0	478.2 ± 14.2	428	478

[a] Values given by manufacturer.
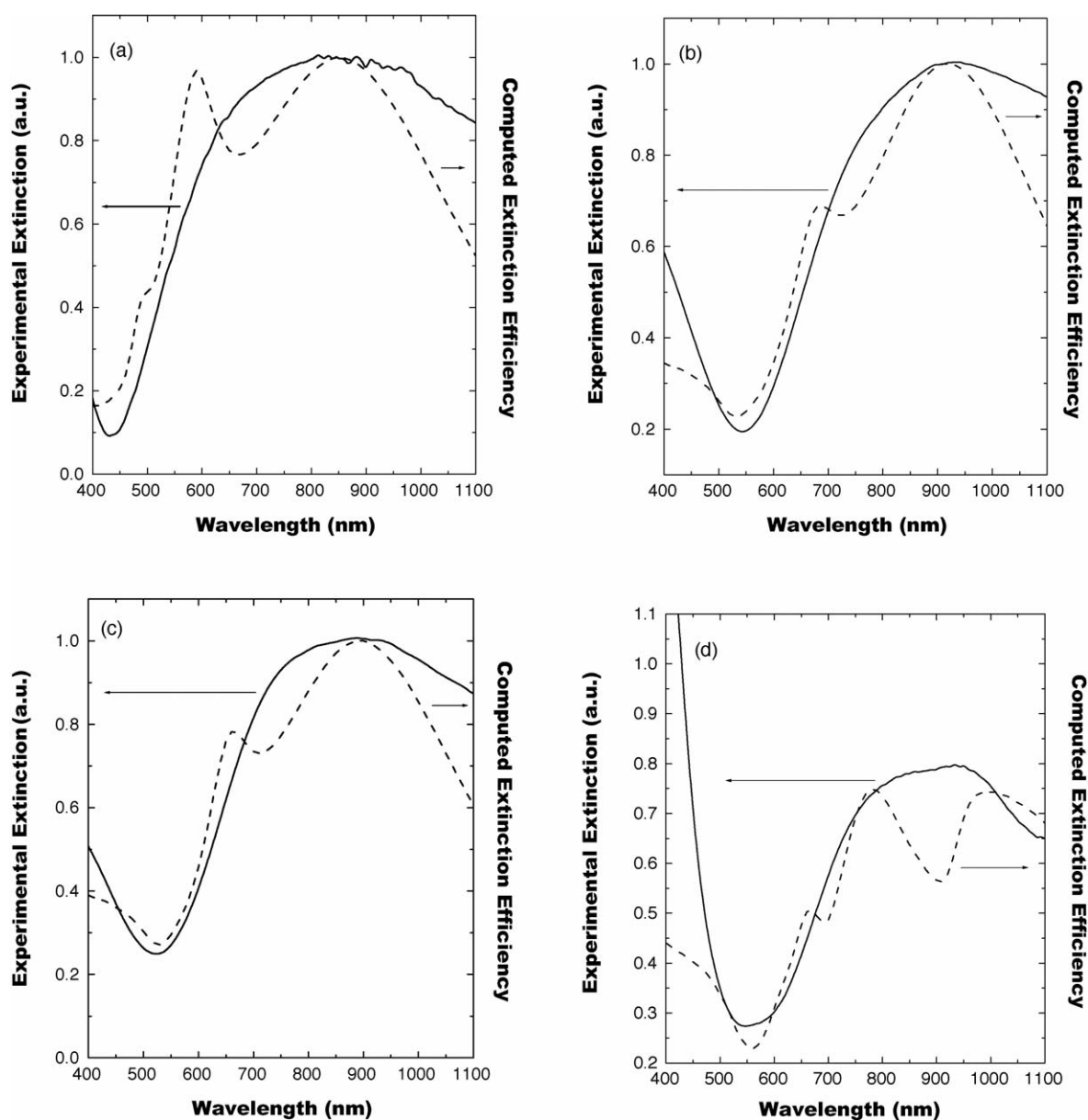[b] Polystyrene particles measured with TEM.

Fig. 22. Comparison of experimental extinction spectra (solid lines) with extended Mie theory calculations (dashed lines) for (a) 168 nm core diameter, 199 nm silver shell diameter; (b) 168 nm core diameter, 196 nm gold shell diameter; (c) 168 nm core diameter, 201 nm gold shell diameter; and (d) 428 nm core diameter, 478 nm gold shell diameter.

[54–56]. Hollow silver shells may be obtained by direct removal of the polystyrene core, and are potentially useful in drug delivery [57]. The use of polystyrene latex spheres as the dielectric cores in these applications may be advantageous because of their ready commercial availability in a wide range of sizes, with very high monodispersity, and with dyes or other organic molecules incorporated into them. Silver nanoparticles are also well known for their antibacterial properties [58]. Zhang et al. [59] reported that silver-coated TiO_2 (core–shell structure) was a more effective antibacterial material than uncoated TiO_2 under UV irradiation. Therefore, the synthesized gold core–silver shell structure nanoparticles may serve as a potential material for antibacterial and other bio-applications.

4. Conclusion

In summary, gold and silver shells of tunable thickness have been fabricated on polystyrene spheres with diameters ranging from 188 to 543 nm. The carboxylate-terminated polystyrene particles were functionalized with 2-aminoethanethiol hydrochloride (AET) to provide thiol groups on their surface. Two types of gold nanoparticles, ∼2 or ∼12 nm in diameter, were bound to the thiol groups on the polystyrene surface, and served as seeds for the growth of a continuous silver or gold shell. The shell thickness and roughness were controlled by the size of the gold nanoparticle seeds and by the procedure of their growth into a continuous shell. By varying the amount of silver or gold deposited onto the polystyrene core, the plasmon resonance of the nanoshell can be tuned across the visible and near-infrared range of the electromagnetic spectrum. The possibility of tuning the plasmon resonance of silver-on-gold nanostructures without the presence of a dielectric core has also been demonstrated, and is attributed to the formation of necklace-like chain aggregates of silver-coated gold nanoparticles.

Acknowledgements

References

[1] P.N. Prasad, Nanophotonics, Wiley-Interscience, New York, 2004.

[2] H. Itoh, K. Naka, Y. Chujo, Synthesis of gold nanoparticles modified with ionic liquid based on the imidazolium cation, J. Am. Chem. Soc. 126 (2004) 3026–3027.

[3] S. Magdassi, A. Bassa, Y. Vinetsky, A. Kamyshny, Silver nanoparticles as pigments for water-based ink-jet inks, Chem. Mater. 15 (2003) 2208–2217.

[4] D.G. Duff, A. Baiker, I. Gameson, P.P. Edwards, A new hydrosol of gold cluster. 1. Formation and particle-size variation, Langmuir 9 (1993) 2301–2309.

[5] S. Link, M.B. Mohamed, M.A. El-Sayed, Simulation of the optical absorption spectra of gold nanorods as a function of their aspect ratio and the effect of the medium dielectric constant, J. Phys. Chem. B 103 (1999) 3073–3077.

[6] S. Link, Z.L. Wang, M.A. El-Sayed, Alloy formation of gold-silver nanoparticles and the dependence of the plasmon absorption on their composition, J. Phys. Chem. B 103 (1999) 3529–3533.

[7] U. Kreibig, L. Genzel, Optical-absorption of small metallic particles, Surf. Sci. 156 (1985) 678–700.

[8] K.L. Kelly, E. Coronado, L.L. Zhao, G.C. Schatz, The optical properties of metal nanoparticles: the influence of size, shape, and dielectric environment, J. Phys. Chem. B 107 (2003) 668–677.

[9] T.K. Sau, C.J. Murphy, Seeded high yield synthesis of short Au nanorods in aqueous solution, Langmuir 20 (2004) 6414–6420.

[10] S.J. Oldenburg, R.D. Averitt, S.L. Westcott, N.J. Halas, Nanoengineering of optical resonances, Chem. Phys. Lett. 288 (1998) 243–247.

[11] J.P. Novak, C. Nickerson, S. Franzen, D.L. Feldheim, Purification of molecularly bridged metal nanoparticle arrays by centrifugation and size exclusion chromatography, Anal. Chem. 73 (2001) 5758–5761.

[12] R.A. Caruso, M. Antonietti, Sol–gel nanocoating: an approach to the preparation of structured materials, Chem. Mater. 13 (2001) 3272–3282.

[13] M.D. Malinsky, K.L. Kelly, G.C. Schatz, R.P. Van Duyne, Chain length dependence and sensing capabilities of the localized surface plasm on resonance of silver nanoparticles chemically modified with alkanethiol self-assembled monolayers, J. Am. Chem. Soc. 123 (2001) 1471–1482.

[14] F.X. Zhang, L. Han, L.B. Israel, J.G. Daras, M.M. Maye, N.K. Ly, C.-J. Zhong, Colorimetric detection of thiol-containing amino acids using gold nanoparticles, Analyst 127 (2002) 462–465.

[15] Y. Hamanaka, A. Nakamura, N. Hayashi, S. Omi, Dispersion curves of complex third-order optical susceptibilities around the surface plasmon resonance in Ag nanocrystal-glass composites, J. Opt. Soc. Am. B 20 (2003) 1227–1232.

[16] G. Carotenuto, Synthesis and characterization of poly(N-vinylpyrrolidone) filled by monodispersed silver clusters with controlled size, Appl. Organomet. Chem. 15 (2001) 344–351.

[17] J. Pendry, Playing tricks with light, Science 285 (1999) 1687–1688.

[18] B. Knoll, F. Keilmann, Near-field probing of vibrational absorption for chemical microscopy, Nature 399 (1999) 134–137.

[19] P.M. Tessier, O.D. Velev, A.T. Kalambur, J.F. Rabolt, A.M. Lenhoff, E.W. Kaler, Assembly of gold nanostructured films templated by colloidal crystals and use in surface-enhanced raman spectroscopy, J. Am. Chem. Soc. 122 (2000) 9554–9555.

[20] P. Das, H. Metiu, Enhancement of molecular fluorescence and photochemistry by small metal particles, J. Phys. Chem. 89 (1985) 4680–4687.

[21] J.J. Storhoff, R. Elghanian, R.C. Mucic, C.A. Mirkin, R.L. Letsinger, One-pot colorimetric differentiation of polynucleotides with single base imperfections using gold nanoparticle probes, J. Am. Chem. Soc. 120 (1998) 1959–1964.

[22] N.J. Halas, The optical properties of nanoshells, Opt. Photonics News (2002) 26–30.

[23] Y. Kobayashi, V. Salgueirino-Maceira, L.M. Liz-Marzan, Deposition of silver nanoparticles on silica spheres by pretreatment steps in electroless plating, Chem. Mater. 13 (2001) 1630–1633.

[24] T. Pham, J.B. Jackson, N.J. Halas, T.R. Lee, Preparation and characterization of gold nanoshells coated with self-assembled monolayers, Langmuir 18 (2002) 4915–4920.

[25] J.L. West, N.J. Halas, Applications of nanotechnology to biotechnology—commentary, Curr. Opin. Biotech. 11 (2000) 215–217.

[26] C. Charnay, A. Lee, S.-Q. Man, C.E. Moran, C. Radloff, R.K. Bradley, N.J. Halas, Reduced symmetry metallodielectric nanoparticles: chemical synthesis and plasmonic properties, J. Phys. Chem. B 107 (2003) 7327–7333.

[27] S.J. Oldenburg, S.L. Westcott, R.D. Averitt, N.J. Halas, Surface enhanced Raman scattering in the near infrared using metal nanoshell substrates, J. Chem. Phys. 111 (1999) 4729–4735.

[28] J.H. Zhang, J.B. Liu, S.Z. Wang, P. Zhan, Z.L. Wang, N.B. Ming, Facile methods to coat polystyrene and silica colloids with metal, Adv. Funct. Mater. 14 (2004) 1089–1096.

[29] P.P.T. Markowicz, H. Pudavar, P.N. Prasad, N.N. Lepeshkin, R.W. Boyd, Dramatic enhancement of third-harmonic generation in three-dimensional photonic crystals, Phys. Rev. Lett. 92 (2004), 083903 (083901–083904).

[30] H. Tiryaki, K. Baba, P.P. Markowicz, P.N. Prasad, Linear and nonlinear optical studies in photonic crystal alloys, Opt. Lett. 29 (2004) 2276–2278.

[31] W. Shi, Y. Sahoo, T. Swihart, P.N. Prasad, Gold nanoshells on polystyrene cores for control of surface plasm on resonance, Langmuir 21 (2005) 1610–1617.

[32] Z.-J. Jiang, C.-Y. Liu, Seed-mediated growth technique for the preparation of a silver nanoshell on a silica sphere, J. Phys. Chem. B 107 (2003) 12411–12415.

[33] A.G. Dong, Y.J. Wang, Y. Tang, N. Ren, W.L. Yang, Z. Gao, Fabrication of compact silver nanoshells on polystyrene spheres through electrostatic attraction, Chem. Commun. 4 (2002) 350–351.

[34] C. Song, D. Wang, Y. Lin, Z. Hu, G. Gu, X. Fu, Formation of silver nanoshells on latex spheres, Nanotechnology 15 (2004) 962–965.

[35] A.B.R. Mayer, W. Grebner, R. Wannemacher, Preparation of silver-latex composites, J. Phys. Chem. B 104 (2000) 7278–7285.

[36] P.A. Schueler, J.T. Ives, F. Delacroix, W.B. Lacy, P.A. Becker, J.M. LI, K.D. Caldwell, B. Drake, J.M. Harris, Physical structure, optical resonance, and surfcace-enhanced Raman-scattering of silver-island films on suspended polymer latex-particles, Anal. Chem. 65 (1993) 3177–3186.

[37] P. Zhan, J.B. Liu, W. Dong, H. Dong, Z. Chen, Z.L. Wang, Y. Zhang, S.N. Zhu, N.B. Ming, Reflectivity behavior of two-dimensional ordered array of metallodielectric composite particles at large incidence angles, Appl. Phys. Lett. 86 (2005), 051108.

[38] H.B. Weiser, The Colloidal Elements, Wiley, New York, 1933.

[39] B.V. Enustun, J. Turkevich, Coagulation of colloidal gold, J. Am. Chem. Soc. 85 (1963) 3317–3328.

[40] J.B. Jackson, N.J. Halas, Silver nanoshells: variations in morphologies and optical properties, J. Phys. Chem. B 105 (2001) 2743–2746.

[41] R. Zsigmondy, Kolloidchemie I and II, Spamer, Leipzig, 1927.

[42] Y.T. Lim, O.O. Park, H.-T. Jung, Gold nanolayer-encapsulated silica particles synthesized by surface seeding and shell growing method: near infrared responsive materials, J. Colloid Interface Sci. 263 (2003) 449–453.

[43] C. Graf, A. van-Blaaderen, Metallodielectric colloidal core–shell particles for photonic applications, Langmuir 18 (2002) 524–534.

[44] T. Sato, S. Kuroda, A. Takami, Y. Yonezawa, H. Hada, Photochemical formation of silver-gold composite colloids in solutions containing sodium alginate, Appl. Organomet. Chem. 5 (1991) 261–268.

[45] P. Mulvaney, M. Giersig, A. Henglein, Electrochemistry of multilayer colloids: preparation and absorption spectrum of gold-coated silver particles, J. Phys. Chem. 97 (1993) 7061–7064.

[46] M. Treguer, C. de Cointet, H. Remita, J. Khatouri, M. Mostafavi, J. Amblard, J. Belloni, R. de Keyzer, Dose rate effects on radiolytic synthesis of gold-silver bimetallic clusters in solution, J. Phys. Chem. B 102 (1998) 4310–4321.

[47] J.H. Hodak, A. Henglein, M. Giersig, G.V. Hartland, Laser-induced inter-diffusion in AuAg core–shell nanoparticles, J. Phys. Chem. B 49 (2000) 11708–11718.

[48] Y. Kim, R.C. Johnson, J. Li, J.T. Hupp, G.C. Schatz, Synthesis, linear extinction, and preliminary resonant Hyper-Rayleigh scattering studies of gold-core/silver-shell nanoparticles: comparisons of theory and experiment, Chem. Phys. Lett. 352 (2002) 421–428.

[49] N.R. Jana, L. Gearheart, S.O. Obare, C.J. Murphy, Anisotropic chemical reactivity of gold spheroids and nanorods, Langmuir 18 (2002) 922–927.

[50] K.G. Thomas, S. Barazzouk, B.I. Ipe, S.T.S. Joseph, P.V. Kamat, Uniaxial plasmon coupling through longitudinal self-assembly of gold nanorods, J. Phys. Chem. B 108 (2004) 13066–13068.

[51] A.L. Aden, M. Kerker, Scattering of electromagnetic waves from two concentric spheres, J. Appl. Phys. 22 (1951) 1242–1246.

[52] O.B. Toon, T.P. Ackerman, Algorithms for the calculation of scattering by stratified spheres, Appl. Opt. 20 (1981) 3657–3660.

[53] S.L. Westcott, J.B. Jackson, C. Radloff, N.J. Halas, Relative contributions to the plasmon line shape of metal nanoshells, Phys. Rev. B 66 (2002) 155431–155435.

[54] R. Weissleder, A clearer vision for in vivo imaging, Nat. Biotechnol. 19 (2001) 316–317.

[55] L.R. Hirsch, R.J. Stafford, J.A. Bankson, S.R. Sershen, B. Rivera, R.E. Price, J.D. Hazle, N.J. Halas, West J: nanoshell-mediated near-infrared thermal therapy of tumors under magnetic resonance guidance, Proc. Natl. Acad. Sci. U.S.A. 100 (2003) 13549–13554.

[56] D.P. O'Neal, L.R. Hirsh, N.J. Halas, J.D. Payne, J.L. West, Photo-thermal tumor ablation in mice using near infrared-adsorbing nanoparticles, Cancer Lett. 209 (2004) 171–176.

[57] Z. Liang, A. Susha, F. Caruso, Gold nanoparticle-based core–shell and hallow spheres and ordered assemblies thereof, Chem. Mater. 15 (2003) 3176–3183.

[58] F.-R.F. Fan, A.J. Bard, Chemical, electrochemical, gravimetric, and microscopic studies on antimicrobial silver films, J. Phys. Chem. B 106 (2002) 279–287.

[59] L. Zhang, J.C. Yu, H.Y. Yip, Q. Li, K.W. Kwong, A.-W. Xu, P.K. Wong, Ambient light reduction strategy to synthesize silver nanoparticles and silver-coated TiO_2 with enhanced photocatalytic and bactericidal activities, Langmuir 19 (2003) 10372–10380.